Journal of Materials Science: Materials in Electronics (2020) 31:8556–8563
https://doi.org/10.1007/s10854-020-03391-x

Rational design of SnO_2 nanoflakes as a stable and high rate anode for lithium-ion batteries

D. Narsimulu[1,2] · N. Naresh[1] · B. Nageswara Rao[3] · N. Satyanarayana[1]

Received: 9 September 2019 / Accepted: 10 April 2020 / Published online: 19 April 2020

Abstract

The SnO_2 nanoflakes were prepared by simple one-step facile microwave-assisted solvothermal synthesis. The as-prepared SnO_2 nanoflakes were systematically studied using X-ray diffraction (XRD), field emission scanning electron microscopy (FE-SEM) and high-resolution transmission electron microscopy (HR-TEM). From FE-SEM images seen that SnO_2 nanoparticles are stocked between the SnO_2 nanoflakes and also, pores are existed between the SnO_2 flakes. TEM results reveal that the SnO_2 nanoflakes were formed due to the self-assembly of very thin SnO_2 nanosheets and also pores coexist between the sheets. The prepared SnO_2 nanoflakes are used as an anode material for the fabrication of lithium-ion battery (LIB). The SnO_2 nanoflakes electrode was found to show a stable reversible lithium storage capacity of 567 mA h g^{-1} even at a current density of 500 mA g^{-1} after 50 cycles. The enhanced properties in terms of reversible capacity and cycle ability of the SnO_2 nanoflakes as an anode material are owing to its porous nature, which facilitates more lithium storage and interconnection between the flakes and particles enhance the kinetic properties of the electrode material. Hence, the developed SnO_2 nanoflakes by simple one-step facile microwave-assisted solvothermal synthesis can be a stable and high rate anode material for lithium-ion batteries.

1 Introduction

Lithium-ion batteries (LIBs) have emerged as an inevitable requirement for many applications like portable electronics, hybrid electric vehicles (HEVs), electric vehicles (EVs), smart grids, etc., [1–3]. The properties of LIBs such as high energy density, long life, low cost, etc., compared with other batteries, making them more attractive [1, 4]. The lithium transition metal oxides as cathode and graphite as an anode have been used generally in commercial LIBs [5, 6]. Though the graphite anode shows excellent capacity but hinders wide industrial application owing to its inherent limitation of low theoretical capacity (372 mA h g^{-1}) [2, 6]. Since the electrode materials play an important role towards the development of high energy density, long life, low cost, etc., properties of LIBs. World-wide research has been focusing mainly on the designing of nanostructured electrode materials with different morphology for developing high energy density, long life, low cost, etc., properties of LIBs. In this regard, as an alternative to graphite anode, SnO_2, a large bandgap semiconductor, has attained considerable attention due to its attractive theoretical capacity (792 mA h g^{-1}), non-toxicity and low voltage platform [7–11]. However, its application in practical LIBs is still hindered due to the rapid capacity loss during repeated cycling arising from the large volume expansion induced by lithium insertion/extraction process [9, 11, 12]. To address these issues, many efforts have been made by the researchers to design novel nanostructures of SnO_2-based anodes like nanowires, nanosheets, nanotubes, nano boxes, hollow spheres, mesoporous structures, etc., [8, 13]. Usually, 2D nanostructures materials such as flakes,

Electronic supplementary material The online version of this article (https://doi.org/10.1007/s10854-020-03391-x) contains supplementary material, which is available to authorized users.

✉ D. Narsimulu
dnarsimlu54@gmail.com

✉ N. Satyanarayana
nallanis2011@gmail.com

[1] Department of Physics, Pondicherry University, Puducherry 605014, India

[2] Department of Electronic Engineering, Institute for Wearable Convergence Electronics, Kyung Hee University, 1732 Deogyeong-daero, Giheung-gu, Yongin-si, Gyeonggi-do 17104, Republic of Korea

[3] Division of Physics, Department of Science & Humanities, Vignan's Foundation for Science Technology & Research University, Vadlamudi, AP 522213, India

sheets etc., have enough pores. But these nanostructures exhibit poor conductivity due to improper interconnection between the particle to particle. Constructing the stacking of nanoparticle between the 2D nanostructures efficiently provide the porous network with good electrical conductivity. The synthesis methods play an important role in tailoring the properties of such kind of nanostructured materials with high surface to volume ratio than the bulk materials. Several synthesis methods such as hydrothermal, sol–gel, co-precipitation, hydrolytic, carbothermal reduction, and polymeric precursor, methods have been reported for the preparation of various kinds of SnO_2 nanostructures [8, 9, 14]. However, all these synthesis methods are time-consuming, demands high-temperature conditions and also difficult to control the growth of the required morphology of SnO_2 materials. Microwave-assisted synthesis method can offer to prepare different dimensions, different shapes of highly reproducible SnO_2 unique nanostructures at relatively low temperature and in a short period [14].

In this work, the unique morphology of SnO_2 nanoflakes with the stocking of SnO_2 nanoparticles was rationally fabricated by using simple one-step microwave-assisted solvothermal synthesis. As prepared SnO_2 nanoflakes were characterized using XRD, FE-SEM & TEM to find out their phase and microstructure, respectively. Interconnection between the flakes and particles enhances the kinetic properties of the electrode material. The prepared SnO_2 nanoflakes are used as an anode material for the fabrication of LIB and the developed LIBs are characterized through cyclic voltammetry and charge–discharge measurements to find out the usefulness of the developed SnO_2 nanoflakes as a stable and high rate anode material for LIB application.

2 Experimental

2.1 *Synthesis of SnO_2 nanoflakes*

SnO_2 nanoflakes were prepared by a simple one-step microwave-solvothermal method. The $SnCl_2.2H_2O$ was used as a tin source, whereas, water and ethanol were used as solvents. The $C_2H_3NaO_2$ was used as the base catalyst and the microwave irradiation in the presence of $C_2H_3NaO_2$ can accelerate the hydrolysis reaction, which may result to form SnO_2 nanoflakes. In typical synthesis process, 1.8 g of tin dichloride ($SnCl_2.2H_2O$, Avra chemicals) and 0.676 g of sodium acetate ($C_2H_3NaO_2$, Alfa Acer) were dissolved in the mixture of distilled water (35 mL) and ethanol (35 mL) solution under continuous stirring for 30 min to obtain homogeneous solution. The prepared solution was transferred into a 100 ml capacity of Teflon liner vessel and it was placed in microwave accelerator, operated at a reaction temperature of 160 °C for 30 min. After completion of the reaction, the collected precipitate was washed several times with water and separated using centrifugation by dispersing the washed precipitate in ethanol solvent. The precipitation was dried in an oven at 80 °C for 24 h to obtain SnO_2 powder. The schematic illustration of the microwave-assisted solvothermal process for the preparation process of the SnO_2 nanoflakes and their growth mechanism is shown in Fig. 1.

2.2 Materials characterization

The crystalline phase of the prepared sample was identified by powder X-ray diffractometer (XRD, X'pert PRO, PAN

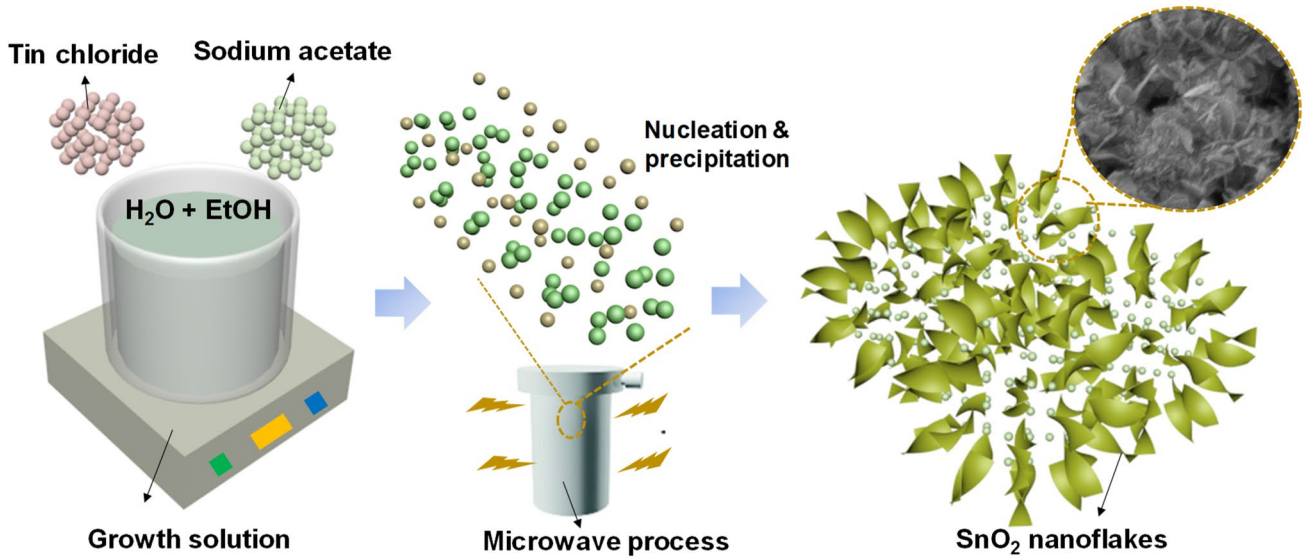

Fig. 1 Schematic illustration of the microwave-assisted solvothermal process for the preparation process of the SnO_2 nanoflakes and their growth mechanism

alytical, Philips) with Cu Kα radiation ($\lambda = 0.154$ nm). The morphology of the prepared sample was obtained using field emission scanning electron microscopy (FE-SEM, SIGMA, ZEISS) and microstructure of the sample was obtained using high-resolution transmission electron microscopy (HR-TEM, TECNAI G20).

2.3 Fabrication and characterization

The composite anode slurry was made by mixing of 70 wt% of SnO_2 powder, 15 wt% of super P carbon, and 15 wt% of poly (vinylidene fluoride) binder in N-methyl 2- pyrrolidone (NMP) solvent. Then, the prepared composite anode slurry was cast on a copper foil using a doctor blade technique followed by drying in a vacuum oven at 120 °C for 12 h. After proper drying, the prepared composite, called a working electrode, was pressed and then cut into circular discs. The coin type LIB was fabricated in an argon-filled glove box (VAC, USA) using components like developed composite electrode material as the working electrode, Lithium metal as the reference electrode, Celgard 2400 as the separator and a solution of $LiPF_6$ (1.0 M) dissolved in 1:1 molar ratio of ethylene carbonate (EC) and diethyl carbonate (DEC) was used as an electrolyte. All the electrochemical measurements like cyclic voltammetry (CV) and galvanostatic charge/discharge (GCD) were performed using an electrochemical system of Bio-Logic Science instruments. The CV measurements were carried out at a scan rate of 0.1 mV s^{-1} at different potential window of 0.001–1.0 V and 0.001–3.0 V. The GCD measurements were carried out at different current densities, and the electrochemical impedance measurements were carried over the frequency range of 0.1–100 k Hz with an amplitude of 5 mV.

3 Results and discussion

3.1 XRD

Figure 2 shows the XRD pattern of the SnO_2 sample. From Fig. 2, all the observed reflections such as (110), (101), (200), (211), (002), (310), (301), (202) and (321) are compared with the tetragonal crystalline phase (JCPDS card no. 41-1445) of SnO_2 and confirmed the formation of pure tetragonal crystalline phase of the prepared SnO_2 sample [15–17]. Also, the crystallite size of the prepared SnO_2 sample is calculated using the measured XRD data and Scherrer formula and it is found to be 15 nm.

3.2 SEM and TEM

The FE-SEM images of the SnO_2 sample at different magnifications are shown in Fig. 3a and b. The high-resolution

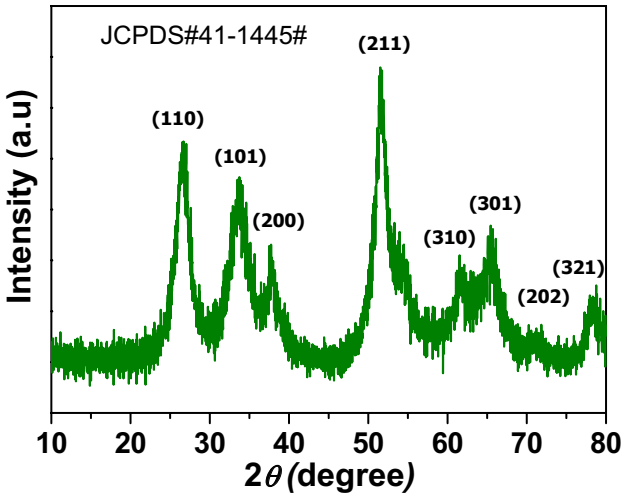

Fig. 2 XRD pattern of as-prepared SnO_2 nanoflakes

of FE-SEM image confirmed that the prepared SnO_2 sample has the nanosized flakes like morphology along with the fine spherical shape nano-size particles. It is seen that the SnO_2 nanoparticles are well-stocked between the SnO_2 nanoflakes and also, pores are existed between the SnO_2 nanoflakes. Figure 3c and d shows the different magnifications of the TEM images of the SnO_2 sample. From Fig. 3c and d, the observed HR-TEM images reveal that the as-prepared SnO_2 nanoflakes are composed of very thin nanosheets with interior pores exist between the nanosheets. The FE-SEM and HR-TEM images results confirmed the interior and exterior pores are present in the SnO_2 nanoflakes sample. This type of pores produce large accessible surface areas, which can act as active sites for better electrochemical reactions. From the inset HR-TEM image of Fig. 3d, the obtained average value of the interplanar spacing of as-prepared SnO_2 nanoflakes is found to be 0.22 nm, which corresponds to (113) plane of the tetragonal crystalline phase of the prepared SnO_2 sample and it well agrees with the interplanar spacing of 0.22 nm obtained from the standard XRD pattern.

3.3 Cyclic voltammetry (CV)

The CV curves of the SnO_2 nanoflakes electrode, for the first six cycles recorded within a potential range of 0.001–1.0 V *vs.* (Li/Li^+) at a scan rate of 0.1 mV s^{-1}, are shown in Fig. 4a. From Fig. 4a, the observed characteristic cathodic and anodic peaks obtained at different potentials can be explained in terms of various electrochemical processes such as solid electrolyte interface (SEI) layer formation and lithium alloying/de-alloying, occurring during charge/discharge cycles of the lithium battery. For the first cycle, observed a cathodic peak at 0.8 V is attributed to the formation of a SEI layer and reduction

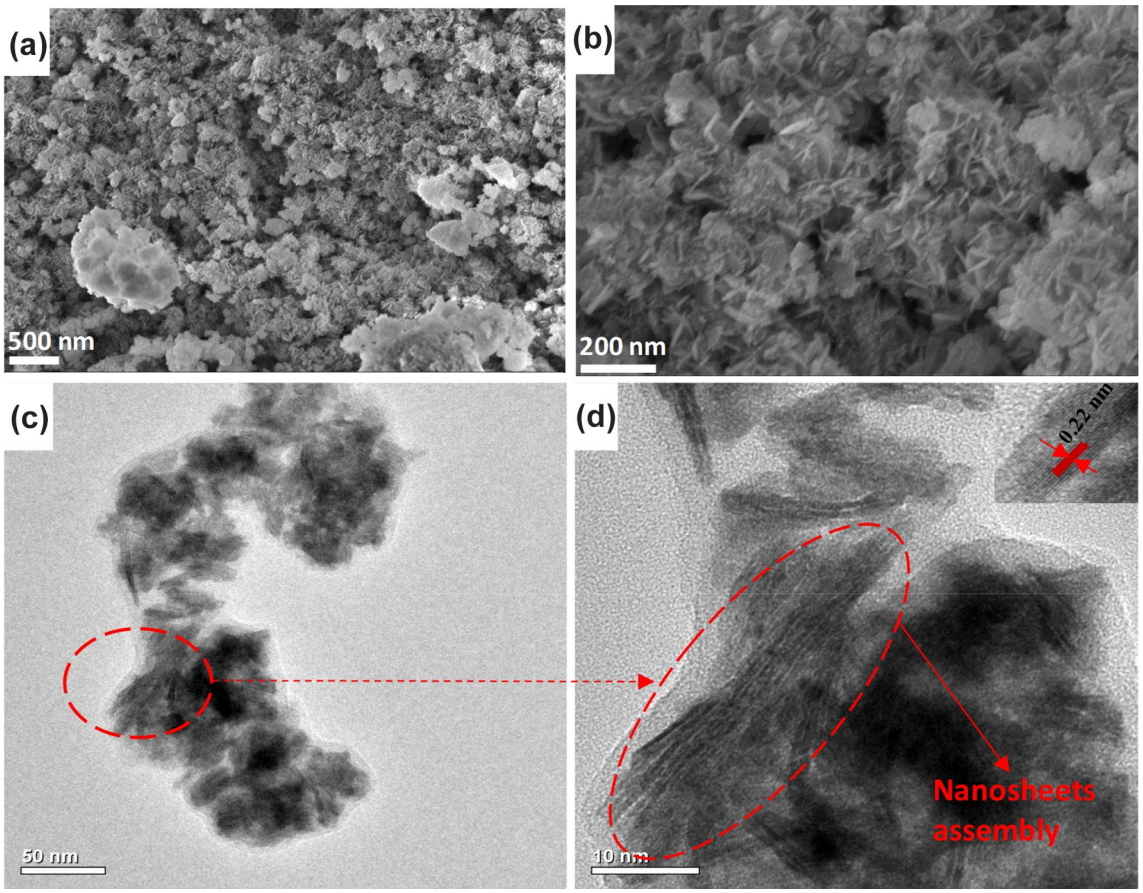

Fig. 3 **a**, **b**, FE-SEM images **c**, **d** TEM images of SnO_2 sample: Inset of 3(d) is the HR-TEM image of SnO_2 sample

of SnO_2 to its metallic form (Sn) [18–20]. After the first cycle, further curves of subsequent cycles are overlapped, indicates the good reversibility of the SnO_2 nanoflakes electrode. The characteristic pair peaks appeared at a potential of 0.04 V (cathodic) and 0.6 V (anodic) [21–24]. These characteristic pair peaks attributed to the alloying (cathodic scan), de-alloying (anodic scan) reactions of lithium with metallic Sn, which is mainly responsible for the reversible storage capacity of tin-based electrode. After the 2nd cycle, for the subsequent cycles, the peak intensity and integrated area almost coincided, indicates the good reversible reaction. For the comparison, we have measured CV curves of SnO_2 between 0.001 and 3.0 V *vs*. (Li/Li^+) at a scan rate of 0.1 mV s^{-1} and are shown in Fig. S1a. As seen in Fig. S1a, the oxidation–reduction behaviour is similar to the CV curves measured between 0.001 and 1.0 V, except the broad anodic peak observed at 0.92–1.5 V. The observed additional broad peak (0.92–1.5 V) may be related to the reversible conversion of Li_2O to Li^+.

3.4 Charge–discharge measurements

The GCD properties of SnO_2 nanoflakes electrode were studied. Figure 4b shows the GCD measurements and Fig. 4c shows the cycling performances of SnO_2 nanoflakes electrode measured at 500 mA g^{-1} for 50 cycles. From Fig. 4b, it is observed that high initial discharge capacity of 1405 mA h g^{-1} and charge capacity of 425 mA h g^{-1}, which results in poor Coulombic efficiency of 30%. The Coulombic efficiency was improved to 80% for second cycle and then 97% after 50 cycles. The large irreversible capacity of about 980 mA h g^{-1} was delivered for the first cycle, which corresponds to the decomposition of electrolyte and formation of the SEI layer on the surface of the electrode [15, 21, 25]. The improved Coulombic efficiency upon continuous cycling corresponds to the formation of a thin and stable SEI layer. It is noteworthy that the specific capacity appeared stable over 50 cycles and found to be 567 mA h g^{-1} and 88% of the capacity is recovered from the 2nd cycle to end of the 50th cycle. The discharge

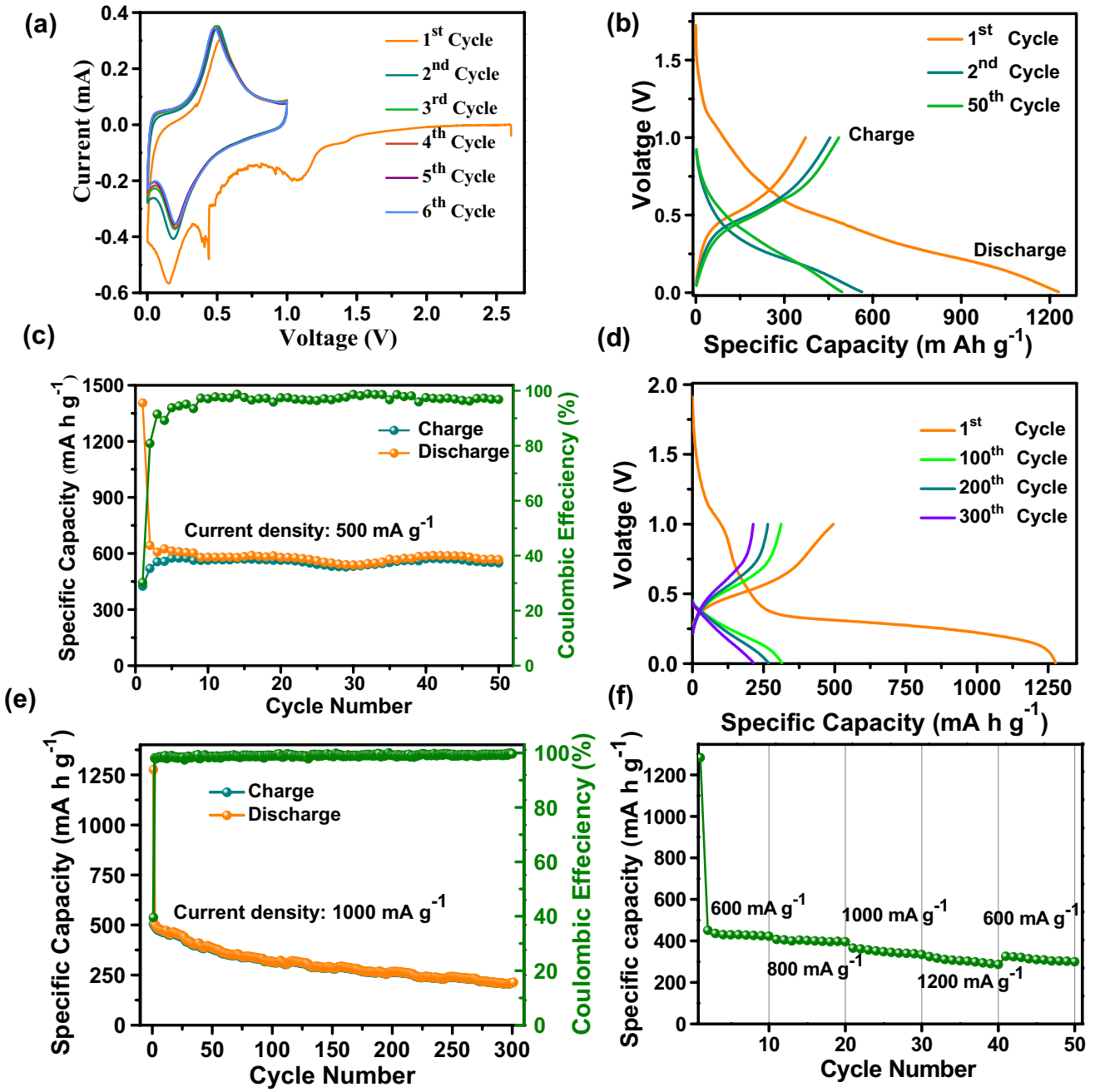

Fig. 4 **a** CV curves of the SnO_2 nanoflakes electrode at a scan rate of 0.1 mV s^{-1}. **b** GCD curves **c** cycling performance of the SnO_2 nanoflakes electrode at 500 mA g^{-1}. **d** GCD curves **e** Cycling performance of the SnO_2 nanoflakes electrode at 1000 mA g^{-1}. **f** Rate performance of the SnO_2 nanoflakes electrode

capacity of SnO_2 electrode after 50 cycles is higher than those of previously reported SnO_2-based electrodes, as seen in Table 1, which is still higher than the theoretical capacity of graphite (372 mA h g^{-1}) [14, 26–33]. Such excellent electrochemical performance in terms of reversibility and rate capability could probably be attributed to the very fine thickness of the sheets and void space between the sheets confirmed by TEM results [34, 35]. In contract, the cycling performance of SnO_2 nanoflakes electrode between 0.05 and 3 V also measured at 500 mA g^{-1} over 50 cycles and shown in Fig. S1b. From Fig. S1b, the obtained discharge capacity only limited to 259 mA h g^{-1} with Coloumbic efficiency of 97%. Figure 4d and e shows the GCD measurements and cycling performance of SnO_2 nanoflakes electrode at a current density of 1000 mA g^{-1} between 0.001 and 1 V. From Fig. 4d, SnO_2 nanoflakes electrode delivered the initial

Table 1 Electrochemical performance of some reported SnO_2-based electrodes with present work

SnO_2-based anode	Preparation process	Final discharge capacity	Current density	References
SnO_2 nanoflakes	Microwave-assisted solvothermal	567 mA h g^{-1}, after 50 cycles 213 mA h g^{-1}, after 300 cycles	500 mA g^{-1} 1000 mA g^{-1}	This work
SnO_2 nanosheets	Microwave-assisted hydrothermal	257 mA h g^{-1}, after 50 cycles	100 mA g^{-1}	[14]
SnO_2 nanoflowers	Microwave-assisted hydrothermal	457 mA h g^{-1}, after 50 cycles	100 mA g^{-1}	[26]
Carbon coated SnO_2 nanotubes	Hydrothermal	400 mA h g^{-1}, after 50 cycles	100 mA g^{-1}	[27]
SnO_2 nanowires	Thermal evaporation	300 mA h g^{-1}, after 50 cycles	100 mA g^{-1}	[28]
SnO_2 nanoparticles	Microwave-assisted hydrothermal	273 mA h g^{-1}, after 100 cycles	100 mA g^{-1}	[29]
SnO_2/reduced graphene oxide	Chemical reduction process	522 mA h g^{-1}, after 50 cycles	160 mA g^{-1}	[30]
SnO_2 carbon fibers	Electrospinning	540 mA h g^{-1}, after 30 cycles	100 mA g^{-1}	[31]
Sn/SnO_2 composite fibers	Electrospinning	445.2 mA h g^{-1}, after 30 cycles	150 mA g^{-1}	[32]
SnO_2/MWCNT	Hydrothermal	344.5 mAh g^{-1}, after 30 cycles	50 mA g^{-1}	[33]

discharge capacity of 1277 mA h g^{-1} and the charge capacity of 506 mA h g^{-1}, respectively, which results in the low Coulombic efficiencies of 40%. After 300 cycles, the delivered discharge capacity of about 213 mA h g^{-1}. The rate performance of anodes in LIB is very essential for high-power required applications such as power grids and electric vehicles.The rate performance of the SnO_2 nanoflakes electrode is shown in Fig. 4f. When the rate capability performed at different current densities of 600, 800, 1000, and 1200 mA g^{-1} delivered discharge capacities of 422, 396, 334, and 286 mA h g^{-1}, respectively. It is worth noting that even at a high current density of 1200 mA g^{-1}, the remarkable reversible capacity of 298 mAh g^{-1} is retained, suggesting an outstanding rate capability of SnO_2 nanoflakes electrode. The enhanced capacity of 300 mA h g^{-1} was achieved when the current rate returns from 1200 to 600 mA g^{-1} after 50 cycles. Further, the specific capacity *vs*. current density of SnO_2 nanoflakes electrode shown in Fig. 5a. From Fig. 5a, there is very less irreversible capacity observed between the initial and final cycles over the different current densities. The rate capability of the electrode was found to be very stable throughout the cycling process. Delivered stable and high capacity of electrode materials at various current densities indicates excellent integrate of the electrode without forming crakes between the SnO_2 nanoflakes throughout the cycling process.

The achieved good electrochemical performance in terms of reversibility and rate performance of the SnO_2 nanosheets anode could be ascribed to the following three reasons: (1) The interior and exterior pores can alleviate mechanical stress caused by the volume variation during charging-discharging processes, as well as provide good contact between the electrode–electrolyte interfaces, (2) interconnection between the flakes and particles enhances

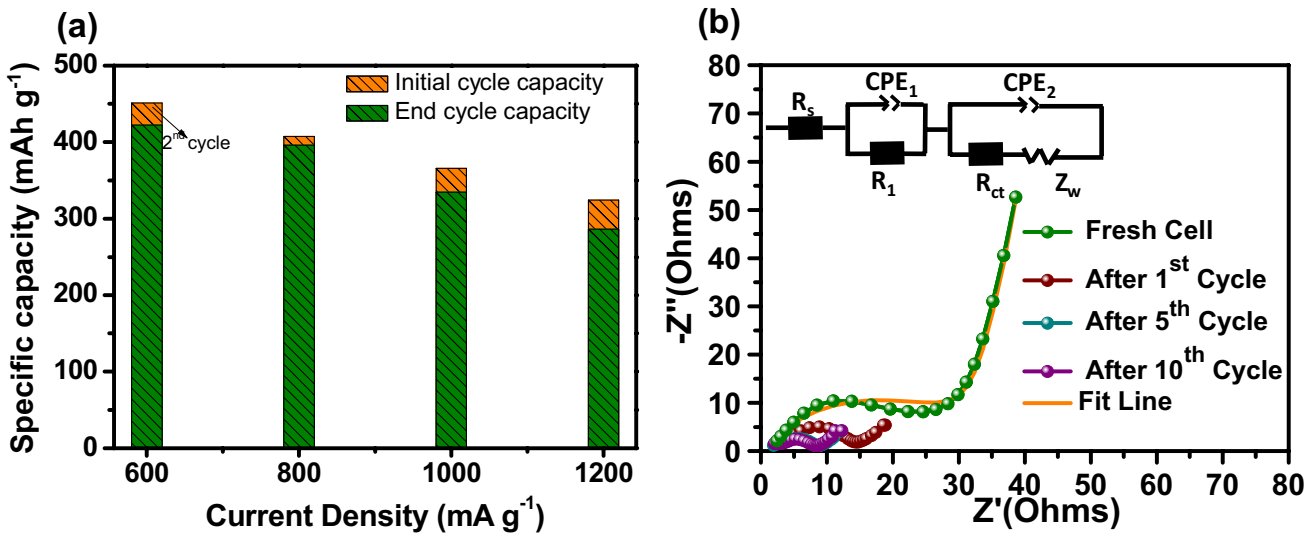

Fig. 5 **a** Specific capacity *vs*. current density and **b** EIS spectra of the SnO_2 nanoflakes electrode

Table 2 Resistances including R_e, R_f, R_{ct} and total resistance (R) of the SnO_2 nanoflakes electrode before and after various cycling

SnO_2 nanoflakes	R_e (Ω)	R_f (Ω)	R_{ct} (Ω)	Total resistance (R) (Ω)
Fresh cell	2.46	4.95	19.2	26.61
After 1st cycle	1.3	2.6	13.4	17.3
After 5th cycle	1.26	4.54	2.15	7.95
After 10th cycle	1.26	4.19	2.56	8.01

the kinetic properties of the electrode material. (3) Ultrafine thickness SnO_2 nanosheets between SnO_2 nanoflakes effectively reduce the Li^+ diffusion length. Hence, confirmed that the developed SnO_2 nanoflakes electrode can be an excellent Li storage capacity.

3.5 Electrochemical impedance spectroscopic (EIS)

The electrochemical charge-transfer kinetics in the SnO_2 material during charge/discharge process was studied using EIS measurements and Fig. 5b shows the impedance plots of SnO_2 nanoflakes electrode for fresh cell, and after 1st, 5th and 10th cycles. The depressed semicircle in the high-frequency region, as observed in Fig. 5b, representing the charge-transfer resistance attributed to the transfer of Li^+ at the electrode and electrolyte interface. Further, the Li^+ mass transfer through diffusion into the electrode material is indicated by the observed sloping line at the low-frequency region. The obtained impedance responses were fitted using BT-Lab software to obtain the electrical equivalent circuit (EEC). The obtained EEC results are shown in the inset of Fig. 5b, and it consists of Ohmic resistance (R_e), surface film resistance (R_f), charge-transfer resistance (R_{ct}), double layer capacitance (CPE), and the Warburg impedance (Z_w). The fitting parameters for after and before cycling are summarized in Table 2. From the Table 2, it is clear that the R_{ct} value is decreasing with the increase in the number charge/discharge cycles suggests the fast charge-transfer process occurring upon continuous cycling [29]. Reduced Rct after 1st cycle may be attributed to SnO_2 nanoparticle trapping between SnO_2 nanoflakes, which acts as a good conductive network and support for fast kinetics of lithium-ions and electrons. Thus, the EIS results revealed the better charge transfers kinetic behaviour of SnO_2 nanoflakes electrode. Hence, the developed SnO_2 nanoflakes by simple one-step facile microwave-assisted solvothermal synthesis can be a stable and high rate anode material for lithium-ion batteries.

4 Conclusion

In summary, SnO_2 nanoflakes were synthesized by a simple and inexpensive one-step microwave-solvothermal method. The prepared SnO_2 nanoflakes exhibit high reversible lithium storage capacity and significantly improved cycling performance. The SnO_2 nanoflakes delivered a high and stable capacity of 567 mA h g^{-1} at a current density of 500 mA g^{-1} over 50 cycles. The demonstrated excellent cycling performance is due to the unique morphology of SnO_2 nanoflakes. The existed interior and exterior pores not sustain the volume changes and also shorten the diffusion length of Li^+. The preparation method is simple, inexpensive and promoting for scaling up to the industrial implementation. Hence, the developed SnO_2 nanoflakes by simple one-step facile microwave-assisted solvothermal synthesis can be a stable and high rate anode material for lithium-ion batteries.

Acknowledgements Prof NS is gratefully acknowledging UGC, Govt. of India for awarding BSR Faculty fellowship: No. F.18-1/2011(BSR), Date: 07-03-2019. Authors also acknowledge CIF, Pondicherry University for using the characterization facilities. Authors are also thankful to Dr.S.M. Shiva Prasad, Professor Jawaharlal Nehru Centre for Advanced Scientific Research (JNCASR) Jakkur, Bangalore-0560064, for providing TEM measurement.

References

1. B. Kang, G. Ceder, Battery materials for ultrafast charging and discharging. Nature **458**, 19–24 (2009)
2. Y. Yao, M.T. Mc Dowell, I. Ryu, H. Wu, N. Liu, L. Hu, W.D. Nix, Y. Cui, Interconnected silicon hollow nanospheres for lithium-ion battery anodes with long cycle life. Nano Lett. **11**, 2949–2948 (2011)
3. H.X. Ji, X.L. Wu, L.Z. Fan, C. Krien, I. Fiering, Y.G. Guo, Y. Mei, O.G. Schmidt, Self-wound composite nanomembranes as electrode materials for lithium-ion batteries. Adv. Mater. **22**, 4591–4595 (2010)
4. G.-L. Xu, S.-R. Chen, J.-T. Li, F.-S. Ke, L. Huang, S.-G. Sun, A composite material of SnO_2/ordered mesoporous carbon for the application in Lithium-Ion Battery. J. Electroanal. Chem **656**, 185–187 (2011)
5. M.S. Dresselhaus, I.L. Thomas, Alternative energy technologies. Nature **414**, 332–336 (2001)
6. Y. Idota, T. Kubota, A. Matsufuji, Y. Maekawa, T. Miyasaka, Tin-Based amorphous oxide: a high-capacity lithium-ion-storage. Mater. Sci. **276**, 1395–1403 (1997)
7. L. Ma, X.-P. Zhou, L.-M. Xu, X.-Y. Xu, L.-L. Zhang, Biopolymer-assisted hydrothermal synthesis of SnO_2 porous nanospheres and their photocatalytic properties. Ceram. Int. **40**, 13659–13667 (2014)
8. H. Bian, J. Zhang, M.-F. Yuen, W. Kang, Y. Zhan, D.Y.W. Yu, Z. Xu, Y.Y. Li, Anodic nanoporous SnO_2 grown on Cu foils as superior binder-free Na-Ion battery anodes. J. Power Sources **307**, 634–637 (2016)
9. M.-S. Park, G.-X. Wang, Y.-M. Kang, D. Wexler, S.-X. Dou, H.-K. Liu, Preparation and electrochemical properties of SnO_2

nanowires for application in Lithium-Ion batteries. Angew. Makromol. Chem. **46**, 750–754 (2007)
10. P. Gurunathan, P.M. Ette, K. Ramesha, Synthesis of hierarchically porous SnO_2 microspheres and performance evaluation as Li-Ion battery anode by using different Binders. ACS Appl. Mater. Interfaces **6**, 16556–16559 (2014)
11. C. Zhang, X. Peng, Z. Guo, C. Cai, Z. Chen, D. Wexler, S. Li, H. Liu, Carbon-coated SnO_2/graphene nanosheets as highly reversible anode materials for Lithium-Ion batteries. Carbon **50**, 1897–1903 (2012)
12. J. Liang, Y. Zhao, L. Guo, L. Li, Flexible free-standing graphene/SnO_2 nanocomposites paper for Li-Ion battery. ACS Appl. Mater. Interfaces **4**, 5742–5747 (2012)
13. S. Han, B. Jang, T. Kim, S.M. Oh, T. Hyeon, simple synthesis of hollow tin dioxide microspheres and their application to Lithium-Ion battery anodes. Adv. Funct. Mater. **15**, 1845–1846 (2005)
14. D. Narsimulu, S. Vinoth, E.S. Srinadhu, N. Satyanarayana, Surfactant-free microwave hydrothermal synthesis of SnO_2 nanosheets as an anode material for lithium battery applications. Ceram. Int. **44**, 201–207 (2018)
15. L. Li, X. Yin, S. Liu, Y. Wang, L. Chen, T. Wang, Electrospun porous SnO_2 nanotubes as high capacity anode materials for lithium ion batteries. Electrochem. Commun. **12**, 1383–1384 (2010)
16. X. Yin, L. Chen, C. Li, Q. Hao, S. Liu, Q. Li, E. Zhang, T. Wang, Synthesis of mesoporous SnO_2 spheres via self-assembly and superior lithium storage properties. Electrochim. Acta **56**, 2358–2366 (2011)
17. P. Lian, X. Zhu, S. Liang, Z. Li, W. Yang, H. Wang, High reversible capacity of SnO_2/graphene nanocomposite as an anode material for Lithium-Ion batteries. Electrochim. Acta **56**, 4532–4538 (2011)
18. Y. Zhu, H. Guo, H. Zhai, C. Cao, Microwave-assisted and gram-scale synthesis of ultrathin SnO_2 nanosheets with enhanced lithium storage properties. ACS Appl. Mater. Interfaces **7**, 2745–2749 (2015)
19. C. He, Y. Xiao, H. Dong, Y. Liu, M. Zheng, K. Xiao, X. Liu, H. Zhang, B. Lei, Mosaic-structured SnO_2@C porous microspheres for high-performance supercapacitor electrode materials. Electrochim Acta **142**, 157–210 (2014)
20. N.R. Srinivasan, S. Mitra, R. Bandyopadhyaya, Improved electrochemical performance of SnO_2–mesoporous carbon hybrid as a negative electrode for lithium ion battery applications. Phys. Chem. Chem. Phys **16**, 6630–6711 (2014)
21. M. Liu, X. Li, H. Ming, J. Adkins, X. Zhao, L. Su, Q. Zhou, J. Zheng, TiN surface-modified SnO_2 as an efficient anode material for lithium ion batteries. New J. Chem. **37**, 2096–2097 (2013)
22. G.Z. Xing, Y. Wang, J.I. Wong, Y.M. Shi, Z.X. Huang, S. Li, H.Y. Yang, Hybrid CuO/SnO_2 nanocomposites: towards cost-effective and high performance binder free lithium ion batteries anode materials. Appl. Phys. Lett **105**, 143905–143906 (2014)
23. X. Zhang, J. Liang, G. Gao, S. Ding, Z. Yang, W. Yu, B.Q. Li, The preparation of mesoporous SnO_2 nanotubes by carbon nanofibers template and their lithium storage properties. Electrochim. Acta **98**, 263–265 (2013)
24. X. Ye, W. Zhang, Q. Liu, S. Wang, Y. Yang, H. Wei, One-step synthesis of Ni-doped SnO_2 nanospheres with enhanced lithium ion storage performance. New J. Chem. **39**, 130–135 (2015)
25. J. Yue, W. Wang, N. Wang, X. Yang, J. Feng, J. Yang, Y. Qian, Triple-walled SnO_2@N-doped carbon@SnO_2 nanotubes as an advanced anode material for lithium and sodium storage. J. Mater. Chem. **3**, 23194–23197 (2015)
26. D. Narsimulu, E.S. Srinadhu, N. Satyanarayana, Surfactant-free microwave-hydrothermal synthesis of SnO_2 flower-like structures as an anode material for lithium-ion batteries. Materialia **4**, 276–286 (2018)
27. P. Wu, N. Du, H. Zhang, J. Yu, Y. Qi, D. Yang, Carbon-coated SnO_2 nanotubes: template-engaged synthesis and their application in lithium-ion batteries. Nanoscale **3**, 746–756 (2011)
28. M.-S. Park, Y.-M. Kang, G.-X. Wang, S.-X. Dou, H.-K. Liu, The effect of morphological modification on the electrochemical properties of SnO_2 nanomaterials. Adv. Funct. Mater **18**, 455–457 (2008)
29. L. Yin, S. Chai, F. Wang, J. Huang, J. Li, C. Liu, X. Kong, Ultrafine SnO_2 nanoparticles as a high performance anode material for lithium ion battery. Ceram. Int. **42**, 9433–9435 (2016)
30. C.-C. Hou, S. Brahma, S.-C. Weng, C.-C. Chang, J.-L. Huang, Facile, low temperature synthesis of SnO_2/reduced graphene oxide nanocomposite as anode material for lithium-ion batteries. Appl. Surf. Sci. **413**, 160–168 (2017)
31. Z. Yang, G. Du, Z. Guo, X. Yu, S. Li, Z. Chen, P. Zhang, H. Liu, Plum-branch-like carbon nanofibers decorated with SnO_2 nanocrystals. Nanoscale **2**, 1011–1017 (2010)
32. D. Narsimulu, S. Vadnala, E. Srinadhu, N. Satyanarayana, Electrospun Sn–SnO_2/C composite nanofibers as an anode material for lithium battery applications. J. Mater. Sci.: Mater. Electron. **29**, 11117–11127 (2018)
33. Z. Wen, Q. Wang, Q. Zhang, J. Li, In Situ growth of mesoporous SnO_2 on multiwalled carbon nanotubes: a novel composite with porous-tube structure as anode for lithium batteries. Adv. Funct. Mater. **17**, 2772–2777 (2007)
34. O. Lupan, L. Chow, G. Chai, A. Schulte, S. Park, H. Heinrich, A rapid hydrothermal synthesis of rutile SnO_2 nanowires. Mater. Sci. Eng. B **157**, 101–104 (2009)
35. J. Yan, E. Khoo, A. Sumboja, P.S. Lee, Facile coating of Manganese oxide on tin oxide nanowires with high-performance capacitive behavior. ACS Nano **4**, 4247–4249 (2010)